Invited Paper

Analysis of Complex Behavior of Stem Cell Populations in Colonic Crypts

Svetoslav Nikolov[1,2,3*], Olaf Wolkenhauer[1,4], Julio Vera[5]

[1]*Department of Systems Biology and Bioinformatics*
University of Rostock, Rostock, Germany
E-mail: olaf.wolkenhauer@uni-rostock.de

[2]*Institute of Mechanics and Biomechanics*
Bulgarian Academy of Sciences
Acad. G. Bonchev Str., Bl. 4, 1113 Sofia, Bulgaria
E-mail: s.nikolov@imbm.bas.bg

[3]*University of Transport*
158 Geo Milev Str., 1574 Sofia, Bulgaria

[4]*Stellenbosch Institute for Advanced Study*
Wallenberg Research Centre at Stellenbosch University
Stellenbosch, South Africa

[5]*Laboratory of Systems Tumor Immunology*
Department of Dermatology
University Hospital Erlangen
Erlangen, Germany
E-mail: jullio.vera-gonzalez@uk-erlangen.de

[*]*Corresponding author*

Received: May 15, 2014 **Accepted: December 22, 2014**

Published: April 20, 2015

Abstract: *Mathematical models of the stem cell populations in colonic crypts can contribute to a better understanding of basic mechanisms underlying tissue organization. We here study the complex dynamic behaviour of a time delay model that describes stem cells in the niche of colonic crypts. We analyze the conditions for the various regimes that would lead to oscillations. The work presented here the first description of a chaotic system describing stem cell population dynamics in colonic crypts.*

Keywords: *Stem cells, Colonic crypts, Time delay model, Nonlinear analysis.*

Introduction

Colorectal cancer (CRC) is a highly prevalent cancer that affects the colon [39, 42, 44]. The colon consists of many millions microscopic structures called *crypts* [3, 12, 34, 38]. At the base of the crypt are located stem cells which are undifferentiated cells. They can keep dividing and undergo an asymmetric differentiation process that transforms some of them into epithelial cells. The differentiating cells travel up the crypt, perform their function, and die by apoptosis after about a week [35, 41, 43]. This relatively short lifespan makes necessary the continuous division of the stem cells at the base to give rise to new differentiated cells in order to replenish the tissue. For this process to be in normal boundaries, it is crucial that the differentiated cells die by apoptosis. If the death of these cells fails, then a dysplastic crypt

appears due to the accumulation of transformed cells around the crypt (formation of a polyp called adenoma). Recent studies of the multi-stage progression of CRC indicate that dysplastic crypt is the first stage of this disease [16, 41]. On the other hand, one of the hypothesized molecular mechanisms linked to the emergence and progression of CRC is a dysfunction in the *Wnt* signalling pathway [21].

A question pertinent to the process of carcinogenesis on the tissue level is the homeostasis of the colonic crypt the balance between cell proliferation and differentiation which ensures that the number of epithelial cells of the crypt lining will remain constant. Under these circumstances, mathematical modeling is a useful tool to better understand the processes involved in carcinogenesis on both the cellular and molecular level. According to [13, 14, 24], there are three common approaches to modeling such processes: compartmental, simulation and stochastic models.

The complex processes in physiology, biology and biochemistry can be described by delay differential equations (DDEs) or more generally functional differential equations when the functional components are affected by physiological or molecular events happened before in the temporal chain of events. Such phenomena are called delay or also genetic effects. Time delays, especially the discrete delays, emerge in various biological contexts [1, 20, 25, 26, 28]. In artificial but also in biological systems, time delayed feedback control is a simple and convenient regulatory structure to stabilize unstable steady states or unstable periodic orbits [19, 31]. In many physiological systems this feedback performs the function of self-regulation. In first order DDEs, the instability arises when the real part of at most one pair of eigenvalues becomes positive [4, 10]. The complex dynamics, as result of mode interactions, is known to occur in these equations when stable 2-tori emerge and delayed feedback loop is included [2, 20].

From mathematical point of view, the delay elements can be considered as a sequence of infinite aperiodic segments. An efficient way of studying an infinite-dimensional system near a bifurcation point is with the help of normal form theory (see Appendix), which consists in transforming a nonlinear system, in order to keep only the relevant nonlinear terms and to allow easier recognition of its dynamics. The center manifold theorem is a powerful result that allows us to drastically reduce the dimension of a problem at a bifurcation point. This theorem also essentially asserts that there is a local (nonlinear) change of coordinates that uncouples the nonlinear terms.

Numerous mathematical models have been proposed to describe stem cell differentiation, amplification and death in the context of colonic crypts. For instance, some investigators have hypothesized that the relationship between cell types in colon crypt compartments will not be constant in strength or direction [36]. These studies include the compartment model proposed by Johnston and co-authors [13, 14], which is used to propose discuss the critical parameters and the underlying reasoning for the hypothesis. The parameters of the age-structured model are the proportions of the number of stem cells in crypt, N_0; the number of semi-differentiated (transit-amplifying) cells, N_1; and the number of fully-differentiated cells, N_2. The compartments and the parameters of the continuous model are the rates of conversion measured in h^{-1}. In Fig. 1, the compartmental model of Johnston is shown.

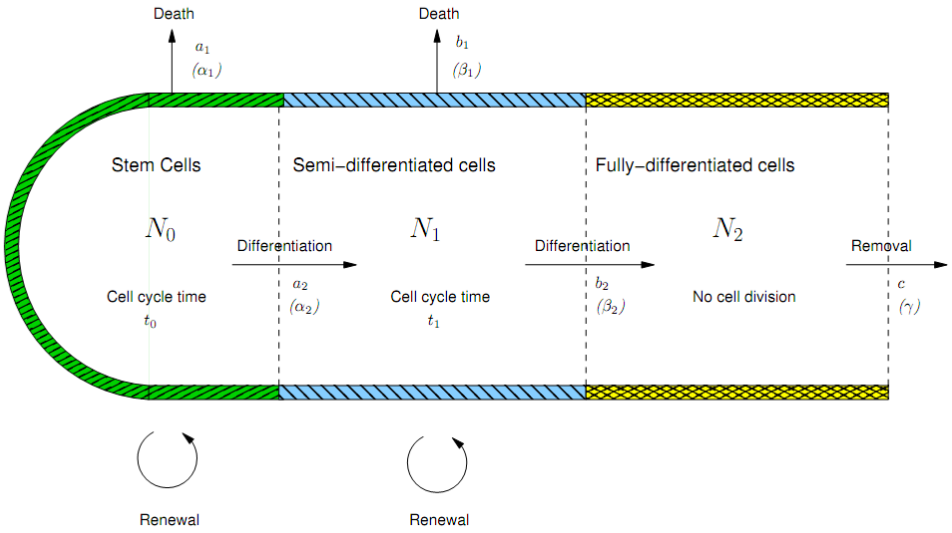

Fig. 1 Illustration of a colonic crypt: stem cells differentiate into semi-differentiated cells, which in turn differentiate into fully-differentiated cells (adapted from [13, 14])

Later, this model was modified by Nikolov et al. [29] with time delays τ_1 and τ_2 for the renewal process of stem and semi-differentiated cells populations (Fig. 2). The time delay model has the form

$$\begin{aligned}
\frac{dN_0}{dt} &= -(\alpha_1+\alpha_2)N_0 + \alpha_3 N_0(t-\tau_2) - \frac{k_0 N_0^2(t-\tau_2)}{1+m_0 N_0(t-\tau_2)},\\
\frac{dN_1}{dt} &= \alpha_2 N_0 - (\beta_1+\beta_2)N_1 + \beta_3 N_1(t-\tau_1) - \frac{k_1 N_1^2(t-\tau_1)}{1+m_1 N_1(t-\tau_1)} + \frac{k_0 N_0^2(t-\tau_2)}{1+m_0 N_0(t-\tau_2)},\\
\frac{dN_2}{dt} &= \beta_2 N_1 - \gamma N_2 + \frac{k_1 N_1^2(t-\tau_1)}{1+m_1 N_1(t-\tau_1)},
\end{aligned} \tag{1}$$

where all variables and parameters are as [13, 14]. On can see that first equation for N_0 into system (1) is independent from the second and the third one. Also, the first two equations in system (1) are independent from the third one. In this paper, we investigate the modified version of first equation in system (1) and identify several different dynamic regimes.

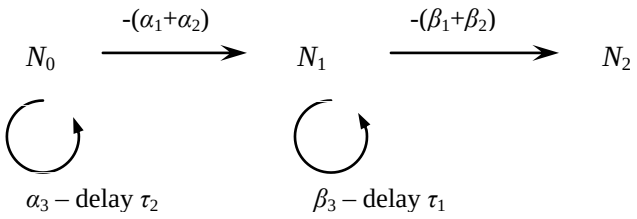

Fig. 2 Saturating feedback.
The maximum per-capita rate of differentiation is assumed.

In [40], stem cells where defined as cells with the capacity for unlimited or prolonged self-renewal that can produce at least one type of highly differentiated descendant. In any

case, it seems obvious that stem cells (or their differentiated progeny) are regulated through mechanisms involving positive and negative feedback loops. According to [6, 37] for Hydra stem cells is experimentally proven that the population size is controlled by negative feedback from the neighbouring cells. Here we assume that when the population size of stem cells increases, the self-renewal rate of the stem cells decrease in order to maintain homeostasis. This leads to a feedback loop in the form

$$\frac{k_0\omega^{l_1}}{\omega^{p_1}+m_0N_0^{l_1}(t-\tau)}, \tag{2}$$

where here $\tau_2 = \tau$. In several experimental and theoretical papers (based on general biological principles) the dependence of the renewal rate on the stem cells density was modelled by a logistic curve [5, 9, 15]. In case that $\omega = 1$, the first differential equation into system (1) has the form

$$\frac{dN_0}{dt} = -(\alpha_1+\alpha_2)N_0 + \alpha_3 N_0(t-\tau) - \frac{k_0 N_0^{l}(t-\tau)}{1+m_0N_0^{l_1}(t-\tau)}, \tag{3}$$

where N_0 is the proportion of the number of stem cells in the crypt; α_i ($i = 1\div3$) are the net per-capita growth rates of the stem cell population; k_0 is nonnegative dimensionless constant which presents the speed of response of the feedback (with large (small) k_0 indicating a fast (slow) feedback response from the system); m_0 is dimensionless constant represent feedback saturation. In the following calculations and simulations we assume that $l = l_1 = 10$.

Qualitative analysis of model (3)

The equilibrium (steady state) points of model (3) can be analytically estimated and are defined by the following set of algebraic equations including the constants of the model:

$$\bar{N}_0^{(1)} = 0,\ \bar{N}_0^{10} - \frac{k_0}{\alpha m_0}\bar{N}_0^{9} + \frac{1}{m_0} = 0, \tag{4}$$

where $\alpha = \alpha_3 - \alpha_1 - \alpha_2$. From a physiological point of view, all equilibrium points must be real non-negative. According to the Descarte's rule [17] the second equation in (4) has always only two real positive roots, which ensure that the system (3) has only three physiologically feasible fixed points.

Investigation of first equilibrium state $\bar{N}_0^{(1)} = 0$

Let us consider a small perturbation (linearization) around the fixed point(s) (4) of the model (3) defined by $N_0 = \bar{N}_0 + x$. Thus, we obtain the original model in local coordinates

$$\dot{x} = -(\alpha_1+\alpha_2)x + \alpha_3 x(t-\tau) - k_0\left(\bar{N}_0 + x(t-\tau)\right)^{10} + k_0 m_0\left(\bar{N}_0 + x(t-\tau)\right)^{20}. \tag{5}$$

Here we note that the feedback loop is expanded as a MacLaurin series, truncated to only linear terms, i.e.

$$\frac{1}{1+\varepsilon} = \frac{1}{1}\left(1-\varepsilon+\varepsilon^2-\varepsilon^3+\ldots\right), \tag{6}$$

where $\varepsilon = m_0\left(\bar{N}_0 + x\left(t-\tau\right)\right)^{10}$.

In case that $\bar{N}_0 = \bar{N}_0^{(1)} = 0$ for Eq. (5) we have

$$\dot{x} = -\alpha_{12}x + \alpha_3 x_\tau - k_0 x_\tau^{10} + k_0 m_0 x_\tau^{20}, \tag{7}$$

where $x_\tau = x(t-\tau)$ and $\alpha_{12} = \alpha_1 + \alpha_2$.

Thus, the characteristic equation of (7) has the form

$$\Delta(\chi) = \chi + \alpha_{12} - \alpha_3 \ell^{-\chi\tau} = 0. \tag{8}$$

Because $\alpha_{12} - \alpha_3 \neq 0$, $\chi = 0$ cannot be a root of Eq. (8) and a stability switch (or cross of the imaginary axis) necessarily occurs with $\chi = in, n > 0$. It is well-known [8] that all roots of Eq. (8) have negative real parts if and only if

$$\tau < 1, \quad \alpha_{12} - \alpha_3 < 0, \quad \alpha_3 \tau > -\xi \sin\xi - \tau\cos\xi, \tag{9}$$

where ξ is the root of $\xi = \tau\tan\xi, 0 < \xi < \pi$, and $\xi = \frac{\pi}{2}$ if $\tau = 0$. Since in our case τ is always positive, the region defined by Eq. (9) is illustrated in Fig. 3 as the hatched one. Therefore, the equilibrium $\bar{N}_0^{(1)} = 0$ in this case is locally asymptotically stable. Because Eq. (8) has a finite number of solutions with zero real part, and all others solutions have negative real part then bifurcations occur for parameter values on these two curves.

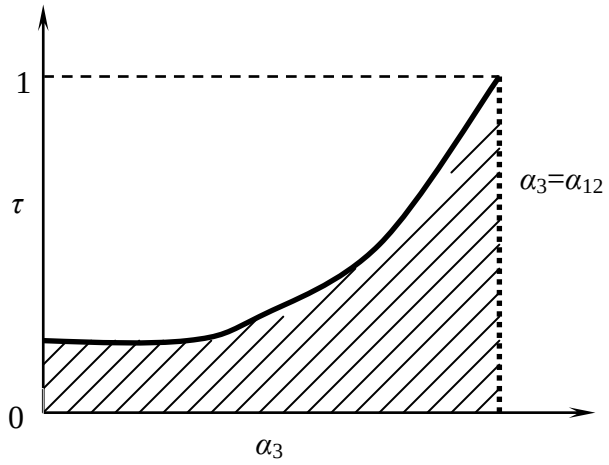

Fig. 3 Stability diagram for the steady state $\bar{N}_0^{(1)} = 0$.
The hatched region corresponds to the region of stability.

The top boundary curve in Fig. 3 is characterized by setting $\chi = in$ into Eq. (5) (i.e. it is an Andronov-Hopf bifurcation curve). After separating Eq. (8) in terms of its real and imaginary parts, we obtain

$$\begin{cases} \alpha_{12} = \alpha_3 \cos n\tau \\ n = -\alpha_3 \sin n\tau \end{cases}. \tag{10}$$

By squaring the two equations into (10) and then adding them, it follows that

$$n = \pm\sqrt{\alpha_3^2 - \alpha_{12}^2}\,. \tag{11}$$

The right-hand boundary curve is characterized by setting $\chi = 0$ in Eq. (8). This substitution gives $\alpha_3 = \alpha_{12}$, i.e. this right boundary line in Fig. 3 is a line where the characteristic Eq. (8) has a single zero root. According to [32] in the point $(\alpha_{12}, \tau) = (\alpha_3, 1)$ where Andronov-Hopf bifurcation curve crosses single zero root line, Eq. (8) has a double zero root and Takens-Bogdanov bifurcation takes place.

To understand the behavior of system (5) near Andronov-Hopf bifurcation (i.e. to understand the stability of the resulting periodic orbits), we need to include the effects of the nonlinear terms of the Eq. (5). We follow the standard procedure, calculating the centre manifold near an arbitrary Andronov-Hopf bifurcation point as a function of *n*.

Let we suppose that (α_0, τ_0) is a point on the top boundary curve in Fig. 3. In this case Eq. (11) has a pair of purely imaginary roots, and all other roots have negative real parts. We rewrite Eq. (10) as

$$\begin{cases} \dfrac{d}{dt}x(t) = -\alpha_{12}x(t) + \alpha_0 x(t-\tau_0) + \mu x(t-\tau_0) - k_0 x^{10}(t-\tau_0) + k_0 m_0 x^{20}(t-\tau_0), \\ \dfrac{d}{dt}\mu(t) = 0, \end{cases} \tag{12}$$

where we have set $\alpha_3 = \mu + \alpha_0$ and $\mu = 0$ is the Andronov-Hopf bifurcation value for Eq. (10).

The linearization of Eq. (12) at the trivial equilibrium is

$$\begin{cases} \dfrac{d}{dt}x(t) = -\alpha_{12}x(t) + \alpha_0 x(t-\tau_0), \\ \dfrac{d}{dt}\mu(t) = 0. \end{cases} \tag{13}$$

A basis for the centre subspace of the linear system (13) can be written in the from

$$\Phi = \begin{pmatrix} \sin(n_0\theta) & \cos(n_0\theta) & 0 \\ 0 & 0 & 1 \end{pmatrix}, \tag{14}$$

where $n_0 = \sqrt{\alpha_0^2 - \alpha_{12}^2}$ by Eq. (11). To determine the coordinates of the centre manifold near the trivial equilibrium, a bilinear form (see (A.6)) reduces to

$$\langle \psi, \phi \rangle = \psi(0)\phi(0) + \alpha_0 \int_{\theta=-\tau_0}^{0} \psi(\zeta + \tau_0) \begin{pmatrix} 1 & 0 \\ 0 & 0 \end{pmatrix} \phi(\zeta) d\zeta . \tag{15}$$

Let

$$\Psi = \left\langle \Phi^{\mathrm{T}}, \Phi \right\rangle^{-1} \Phi^{\mathrm{T}} = \rho \begin{pmatrix} \frac{1}{2}\left[(1-\tau_0)\sin(n_0\theta) + n_0\tau_0\cos(n_0\theta)\right] & 0 \\ \frac{1}{2}\left[-n_0\tau_0\sin(n_0\theta) + (1-\tau_0)\cos(n_0\theta)\right] & 0 \\ 0 & \rho^{-1} \end{pmatrix} \overset{def}{=} \begin{pmatrix} b_1(\theta) & 0 \\ b_2(\theta) & 0 \\ 0 & 1 \end{pmatrix} \tag{16}$$

be a basis for the transposed system to Eq. (13).

Here $\rho = \dfrac{4}{\left[(1-\tau_0)^2 + (n_0\tau_0)^2\right]}$.

It can be easily shown that matrix

$$B = \begin{pmatrix} 0 & -n_0 & 0 \\ n_0 & 0 & 0 \\ 0 & 0 & 0 \end{pmatrix}, \tag{17}$$

satisfies relation (A.10) (see Appendix). Write $z = \left[z_1, z_2, \mu\right]^{\mathrm{T}}$ for the local coordinates on the centre manifold. The nonlinear terms in Eq. (12) are given by

$$F\left(\left[v_1, v_2\right]^{\mathrm{T}}\right) = \left[v_2(0)v_1(-\tau_0) - k_0\left(v_1(-\tau_0)\right)^{10} + k_0 m_0\left(v_1(-\tau_0)\right)^{20}, 0\right]^{\mathrm{T}}. \tag{18}$$

Substituting the results above into (A.9), we obtain the following ordinary differential equations on the centre manifold

$$\begin{aligned} \frac{d}{dt} z_1 &= -n_0 z_2 + b_1(0)\Big[\mu\left(-\sin(n_0\tau_0)z_1 + \cos(n_0\tau_0)z_2\right) - \\ &\quad - k_0\left(-\sin(n_0\tau_0)z_1 + \cos(n_0\tau_0)z_2\right)^{10} + k_0 m_0\left(-\sin(n_0\tau_0)z_1 + \cos(n_0\tau_0)z_2\right)^{20}\Big], \\ \frac{d}{dt} z_2 &= n_0 z_1 + b_2(0)\Big[\mu\left(-\sin(n_0\tau_0)z_1 + \cos(n_0\tau_0)z_2\right) - \\ &\quad - k_0\left(-\sin(n_0\tau_0)z_1 + \cos(n_0\tau_0)z_2\right)^{10} + k_0 m_0\left(-\sin(n_0\tau_0)z_1 + \cos(n_0\tau_0)z_2\right)^{20}\Big], \\ \frac{d}{dt}\mu &= 0. \end{aligned} \tag{19}$$

Now, we consider the linear part (in (z_1, z_2)) of first and second equations into Eq. (19), as we redefine z such that $z = [z_1, z_2]^T$

$$\frac{d}{dt} z = B_1 z, \tag{20}$$

where $B_1 = \begin{pmatrix} -b_1(0)\mu \sin(n_0\tau_0) & -n_0 + b_1(0)\mu\cos(n_0\tau_0) \\ n_0 - b_2(0)\mu\sin(n_0\tau_0) & b_2(0)\mu\cos(n_0\tau_0) \end{pmatrix}$.

In case that $\Delta_1 = (tr(B_1))^2 - 4\det(B_1) < 0$, i.e. the complex eigenvalues take place, we can write $\chi_1 = c_1 + ic_2$ and $\chi_2 = c_1 - ic_2$, where $c_1 = \frac{1}{2} tr(B_1) = \frac{1}{2}\mu[b_2(0)\cos(n_0\tau_0) - b_1(0)\sin(n_0\tau_0)]$ and $c_2 = \frac{1}{2}\sqrt{(-\Delta_1)}$. Hence, the matrix B_1 can be brought into the following Jordan normal (canonical) form $B_2 = \begin{pmatrix} c_1 & -c_2 \\ c_2 & c_1 \end{pmatrix}$. It is seen that the eigenvalue crossing speed $\left.\frac{\partial c_1}{\partial \mu}\right|_{\mu=0}$ on the Hopf curve is positive, so the crossing condition is always satisfied.

Investigation of the equilibrium state $\bar{N}_0 \neq 0$

In this case for the system (5) we have

$$\dot{x} = -\alpha_{12} x + \gamma_1 x_\tau + \gamma_2 x_\tau^2 + \gamma_3 x_\tau^3 + \gamma_4 x_\tau^4 + \ldots \quad h.o.t., \tag{21}$$

where

$$\begin{aligned} &\gamma_1 = \alpha_3 + 10k_0\bar{N}_0^9\left(2m_0\bar{N}_0^{10} - 1\right), \quad \gamma_2 = 5k_0\bar{N}_0^8\left(38m_0\bar{N}_0^{10} - 9\right), \\ &\gamma_3 = 60k_0\bar{N}_0^7\left(19m_0\bar{N}_0^{10} - 2\right), \quad \gamma_4 = 15k_0\bar{N}_0^6\left(323m_0\bar{N}_0^{10} - 14\right). \end{aligned} \tag{22}$$

Thus, the characteristic equation becomes

$$\Delta(\chi) = \chi + \alpha_{12} - \gamma_1 \ell^{-\chi\tau} = 0. \tag{23}$$

We hereafter use the same method of the previous section. Hence, we rewrite Eq. (23) as

$$\left|\begin{aligned} &\frac{dx}{dt} = -\alpha_{12}x(t) + \alpha_0 x(t-\tau_0) + \mu x(t-\tau_0) + \gamma_2\left(x(t-\tau_0)\right)^2 + \gamma_3\left(x(t-\tau_0)\right)^3 + \\ &\qquad + \gamma_4\left(x(t-\tau_0)\right)^4 + O\left(\left|x(t-\tau_0)\right|\right)^5, \\ &\frac{d}{dt}\mu(t) = 0. \end{aligned}\right. \tag{24}$$

The nonlinear terms in Eq. (24) are given by

$$F\left(\left[v_1, v_2\right]^{\mathrm{T}}\right)=\left[v_2(0)v_1(-\tau_0)+\gamma_2\left(v_1(-\tau_0)\right)^2+\gamma_3\left(v_1(-\tau_0)\right)^3+\gamma_4\left(v_1(-\tau_0)\right)^4+O\left(|v|^5\right), 0\right]^{\mathrm{T}}. \quad (25)$$

Substituting the results above into (A.9), we obtain the following ordinary differential equations on the centre manifold

$$\begin{aligned}
\frac{d}{dt}z_1 &= -n_0 z_2 + b_1(0)\Big[\mu\left(-\sin\left(n_0\tau_0\right)z_1+\cos\left(n_0\tau_0\right)z_2\right)+\gamma_2\left(-\sin\left(n_0\tau_0\right)z_1+\cos\left(n_0\tau_0\right)z_2\right)^2+ \\
&\quad +\gamma_3\left(-\sin\left(n_0\tau_0\right)z_1+\cos\left(n_0\tau_0\right)z_2\right)^3\Big], \\
\frac{d}{dt}z_2 &= n_0 z_1 + b_2(0)\Big[\mu\left(-\sin\left(n_0\tau_0\right)z_1+\cos\left(n_0\tau_0\right)z_2\right)+\gamma_2\left(-\sin\left(n_0\tau_0\right)z_1+\cos\left(n_0\tau_0\right)z_2\right)^2+ \\
&\quad +\gamma_3\left(-\sin\left(n_0\tau_0\right)z_1+\cos\left(n_0\tau_0\right)z_2\right)^3\Big], \\
\frac{d}{dt}\mu &= 0.
\end{aligned} \quad (26)$$

After a nonlinear change of variables the equations on the centre manifold can be brought into normal form and truncated at third order to give

$$\frac{d}{dt}z_1=\left(c_1+a\left(z_1^2+z_2^2\right)\right)z_1-\left(c_2+b\left(z_1^2+z_2^2\right)\right)z_2, \quad (27)$$

$$\frac{d}{dt}z_2=\left(c_2+b\left(z_1^2+z_2^2\right)\right)z_1+\left(c_1+a\left(z_1^2+z_2^2\right)\right)z_2, \quad (28)$$

where $a\left(n_0,\tau_0,\alpha_0,\mu,\gamma_1-\gamma_4\right)$ and $b\left(n_0,\tau_0,\alpha_0,\mu,\gamma_1-\gamma_4\right)$ are constants, and are such that Eq. (10) is satisfied.

Eqs. (27) and (28) are a normal form for the standard Hopf bifurcation provided that the first Lyapunov coefficient $a(0)$ and the eigenvalue crossing speed $\left.\frac{\partial c_1}{\partial\mu}\right|_{\mu=0}$ are both finite and non-zero [8, 32].

Numerical analysis

In the previous section, we proposed the analytical tools and used them for a qualitative analysis of the system, obtaining predictions about dynamics (stability and non-regularity) of the system. In this section, we perform a numerical analysis of model (3), based on the results previously obtained. The parameter values used in the numerical analysis were selected according to [13, 14, 20, 27, 42]. However, we do not know the exact time point at which the stem cells begin to renew and assume that they take a little bit longer; hence, we set $\tau \in [1, 33]$ hours [42]. The analytical results stated in the previous section permit us to predict how the properties of the system vary as the parameters in the model (3) are modified.

In Fig. 4a, the stable solution for the number N_0 of stem cells in the crypt is shown for $\tau = 1$. It is evident that after several (fast fluctuations) for stem cells in the crypt, the number N_0 approaches a constant value (equilibrium state). In other words, in this case, the steady states of system (3) are locally asymptotically stable and time delay τ is lower than the critical one.

Here we note that the governing equation of the model, represented by Eq. (3), was solved numerically using MATLAB [22], when the system is with saturating feedback in stem cells, i.e. we used the following fixed values for the system parameters:

$$a_1 = 0.1,\ a_2 = 0.3,\ a_3 = 0.69,\ k_0 = m_0 = 0.1,\ l = l_1 = 10. \quad (29)$$

On the other hand, Fig. 4b depicts the dynamics for the case of time delay higher than the critical value τ_b. We observe oscillating solutions, with period falling in the range of 11 hours to 14 hours. This behavior is in accordance with the data in [13, 14] (and references there in), where the stem cells are assumed to have a cycle time of between 12 and 32 h with an average of 24 h. Mathematically, this state corresponds to a loss of stability. According to analytical results obtained in previous section we can conclude that stable limit cycle (self-oscillations) occurs after an Andronov-Hopf bifurcation. From biological point of view, the occurrence of oscillations with period one implies that stem cells populations is in normal condition, but not robust.

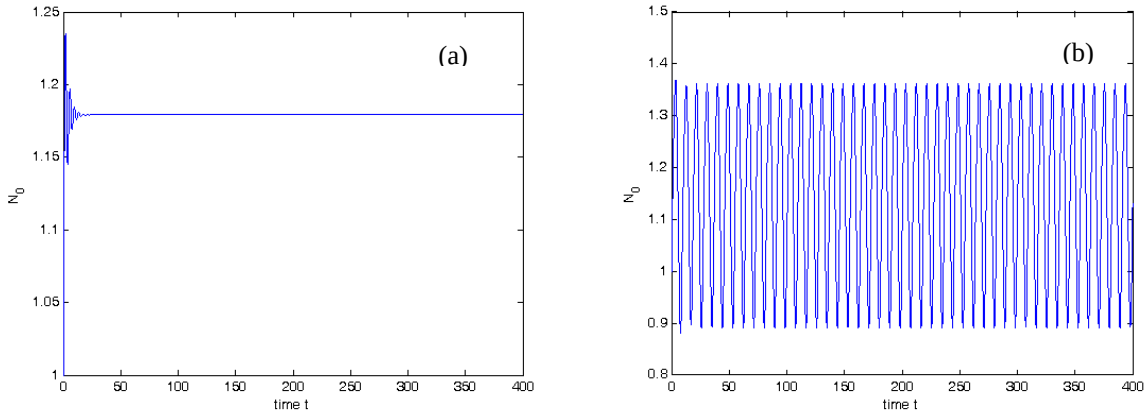

Fig. 4 Stable and periodic solution of the system (3) at: (a) $\tau = 1$ and (b) $\tau = 3$.
Here we note that in both cases $l = l_1 = 10$ and the time is in hours.

Figs. 5 and 6 demonstrate the dependence of oscillations period on the time delay τ. Comparing Fig. 5 and Fig. 6 we see that for smaller value $\tau = 5.1$ the period of oscillations is also smaller with respect to those obtained at $\tau = 6.1$ in Fig. 6. The magnitude of N_0 becomes approximately equal in both cases. From a bifurcation point of view, the secondary Hopf bifurcation takes place and the system (3) has oscillations for $\tau = 6.1$ with period three.

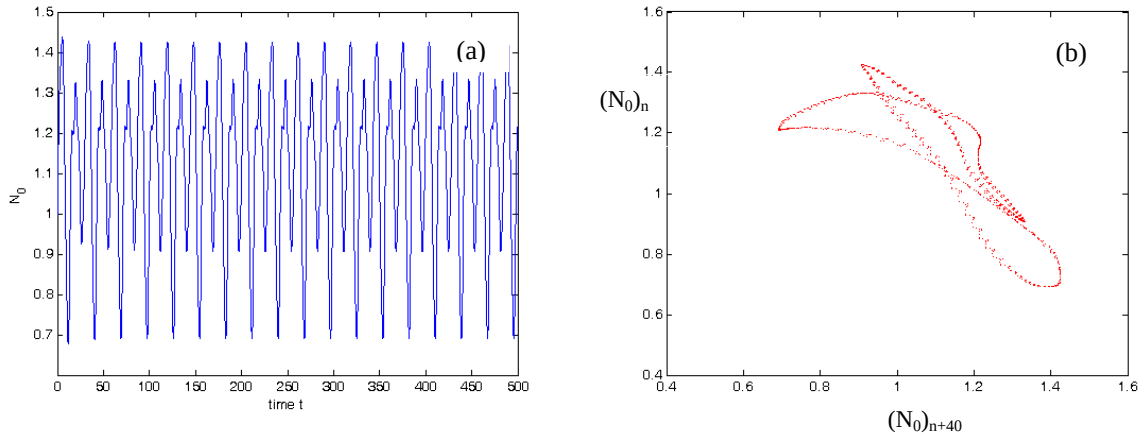

Fig. 5 Dynamic behaviour of system (3) for $\tau = 5.1$
(a) unstable regime (oscillations with period two), (b) phase space

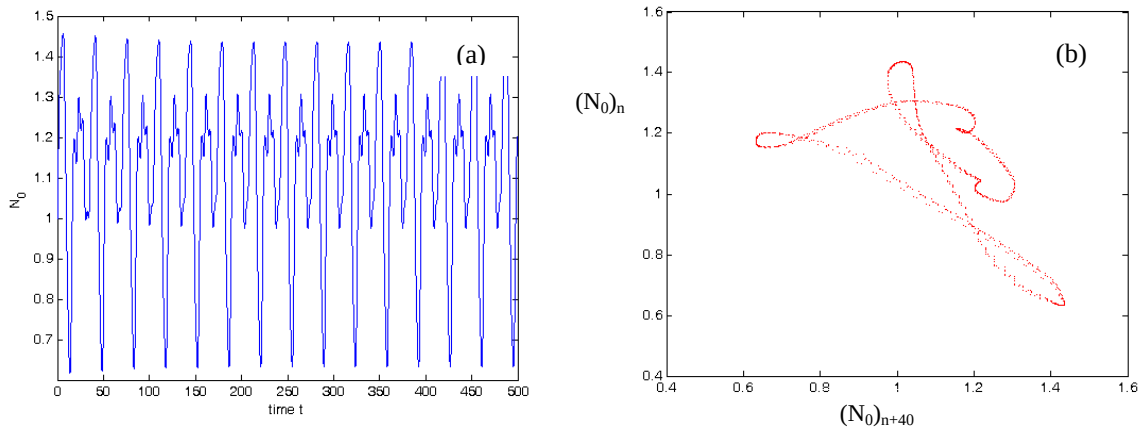

Fig. 6 Dynamic behaviour of system (3) for $\tau = 6.1$
(a) unstable regime (oscillations with period three), (b) phase space

In Fig. 7 we show that system (3) is capable of producing chaotic behaviour too, for values of time delay τ larger than 13.

Chaotic motions are based on homoclinic (heteroclinic) structures with instability accompanied by local divergence and global contraction. Meanwhile, the transition from stability to instability requires the vanishing of stable equilibrium states and of stable periodic motions or sufficiently large increase in the periodic ones [7, 18, 23, 33].

Stable periodic motions and equilibrium states can lose stability or vanish only in several specific ways [23], i.e., we can speak of different routes to chaos: (i) either a stable equilibrium state or a periodic motion merges with the corresponding unstable motion, and then both states vanish; (ii) either an equilibrium state or a periodic motion loses stability, simultaneously generating a stable periodic motion or a stable two-dimensional toroidal manifold with periodic or quasi-periodic coil, respectively; (iii) a stable periodic motion either contracts to a point, generating a stable equilibrium, or merges with an equilibrium, or merges with an equilibrium, generating a doubly asymptotic curve (being the intersection of its integral manifolds W^+ and W^-); (iv) a periodic motion loses stability, simultaneously generating a stable periodic motion with period twice as large. The stability loss can be repeated many times, forming an infinite period-doubling (tripling) bifurcation series. This model demonstrates a period-doubling route to chaos (iii). As one increases τ from $\tau = 3$ (till $\tau = 5$), system (3) has oscillations with period one. As τ increases further, the period-tripling bifurcations occur and at $\tau > 5.1$ (to $\tau = 8.6$) the system has only solutions with period two and three. Finally, at $\tau > 12.6$ (after period doubling bifurcations) the system's behavior becomes chaotic.

A confirmation of our conclusions is the results shown in Fig. 7 and the obtained maximal Lyapunov exponent (per unit time) $\lambda_{max} = +0.0475 \pm 0.026$ at $\tau = 13$. For the numerical calculation of λ_{max}, we use the TISEAN software package [11]. The bifurcation diagram of system (3) in the interval $\tau \in [3, 33]$, is shown in Fig. 8.

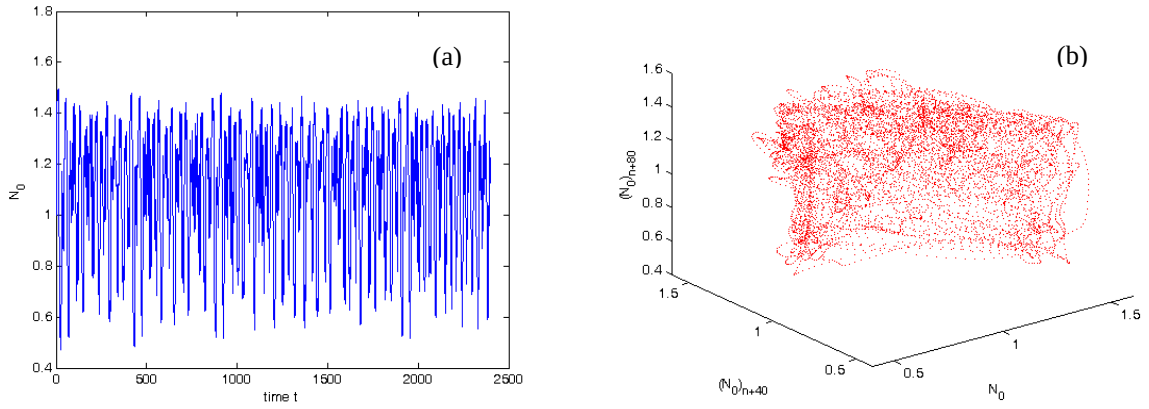

Fig. 7 Time evolution of stem cell population
(a) chaotic behavior, (b) phase space (strange attractor) of system (3) at $\tau = 13$, $l = l_1 = 10$

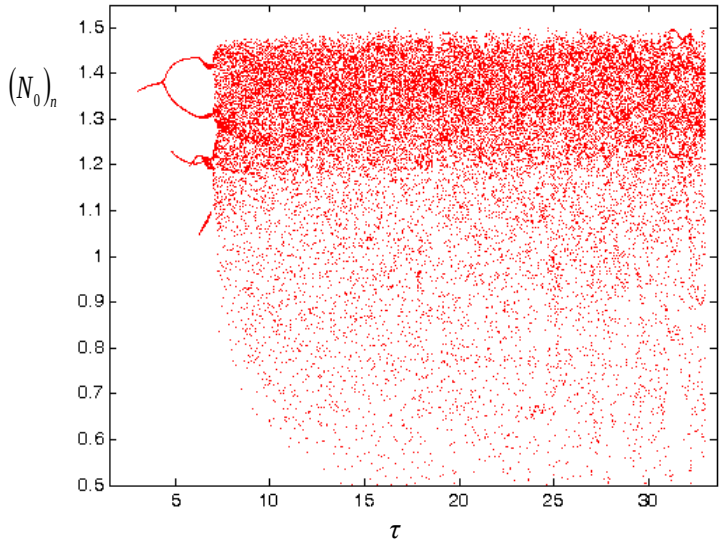

Fig. 8 Bifurcation diagram $(N_0)_n$ versus τ generated by computer solution of system (1) at $l = l_1 = 10$, $a_1 = 0.1$, $a_2 = 0.3$, $a_3 = 0.69$, $k_0 = m_0 = 0.1$. Note that $\tau \in [3, 33]$.

The chaotic behaviour shown in Figs. 7 and 8 require additional comments. Experiments with chimeric mice and with mutagen agents have shown that crypts, initially polyclonal for one marker, eventually become monoclonal, which suggests that symmetric division occasionally occurs and leads to a niche succession by stochastic (non-regular) extinction of stem cell lineages [25]. The stem cell population dynamics in human colon crypt is of interest to cancer because: 1) the stochastic processes are the same in all crypts, except for the age of the crypts; 2) the number of stem cells is stable and the loss of a stem cell is compensated by the symmetric division of one of the other stem cells. Stem cell losses are not compensated by new stem cells originating from another layer of stem cells. These assumptions are intended to be as reasonable as possible, and the demonstration that data are compatible with our simple model (3). Hence, we can formulate the hypothesis that chaotic behaviour of stem cells population in human colon crypts is characteristic of *before pathological (cancer) condition*.

Conclusions

Despite a number of studies reporting the occurrence of various chaotic cancer structures, there is yet little known about mechanisms underlying bifurcation scenarios, which could give rise to clinically observed chaotic patterns. Additionally, little is known about how such patterns are embedded in the parameter space of the cancer models with so-called strange (chaotic) attractors. The reader can find a wealth of information on this in the original paper [30].

In this work we investigated a time delay model of stem cells populations in human colonic crypts. The presented time delay model is the first construction of a chaotic system representing stem cell population dynamics in colonic crypts.

A major motivation for development and investigation of this time delay model is the stimulation of further theoretical and experimental studies aimed at forming progressively more complete and accurate models of the complex process of colon cancer.

References

1. Adimy M., F. Crauste, S. Ruan (2006). Periodic Oscillations in Leucopoiesis Models with Two Delays, J Theor Biol, 242, 288-299.
2. Berger B., M. Rokni, I. Minis (1993). Complex Dynamics in Metal Cutting, Quart Appl Math, 51, 601-612.
3. Boursi B., N. Alber (2007). Current and Future Clinical Strategies in Colon Cancer Prevention and the Emerging Role of Chemoprevention, Curr Pharm Des, 13, 2274-2282.
4. Campbell S., J. Belair, T. Ohira, J. Milton (1995). Limit Cycles, Tori and Complex Dynamics in a Second-order Differential Equation with Delayed Negative Feedback, J Dynamics and Differential Equations, 7, 213-236.
5. Clarke P. (1990). Developmental Cell Death: Morphological Diversity and Multiple Mechanisms, Anat Embryol, 181, 195-213.
6. Di Garbo A., M. Johnston, S. Chapman, P. Maini (2010). Variable Renewal Rate and Growth Properties of Cell Populations in Colon Crypts, Physical Review E, 81, 061909.
7. Gonchenko S., L. Shilnikov, D. Turaev, D (1996). Dynamical Phenomena in Systems with Structurally Unstable Poincare Homoclinic Orbits, Chaos, 6(1), 15-31.
8. Hale J. K., S. M. Verduyn Lunel (1993). Introduction to Functional Differential Equations, Appl Math Sciences, 99, Springer-Verlag, New York.
9. Hardy K., J. Stark (2002). Mathematical Models of the Balance between Apoptosis and Proliferation, Apoptosis, 7(4), 373-381.
10. Hayes N. (1950). Roots of the Transcendental Equation Associated with a Certain Difference-Differential Equations, J London Math Soc, 25, 226-232.
11. Hegger R., H. Kantz, T. Schreiber (1999). Practical Implementation of Nonlinear Time Series Methods: The TISEAN Package, Chaos, 9, 413-435.
12. Humphries A., N. Wrigth (2008). Colonic Crypt Organization and Tumorigenesis, Nature Reviews Cancer, 8, 415-424.
13. Johnston M., C. Edwards, W. Bodmer, P. Maini, S. Chapman (2007). Mathematical Modelling of Cell Population Dynamics in the Colon Cancer Initiation, Proc Nat Acad Sci USA, 104, 4008-4013.
14. Johnston M., C. Edwards, W. Bodmer, P. Maini, S. Chapman (2007). Examples of Mathematical Modelling: Tales from the Crypt, Cell Cycle, 6(17), 2106-2112.
15. Kilian H., D. Bartkowiak, D. Kaufmann, R. Kemkemer (2008). The General Growth Logistics of Cell Populations, Cell Biochem and Biophys, 51(2-3), 51-66.
16. Kinzler K., B. Vogelstein (1998). The Genetic Basis of Cancer, Toronto, McGraw-Hill.

17. Korn G., T. Korn (1968). Mathematical Handbook for Scientists and Engineers, McGraw-Hill Book Company.
18. Kuznetsov S. (2002). Torus Fractalization and Intermittency, Phys Rev E, 65, 066209.
19. Lehnert J., P. Hovel, V. Flunkert, P. Guzenko, A. Fradkov, E. Scholl (2011). Adaptive Tuning of Feedback Gain in Time-delayed Feedback Control, Chaos, 21, 043111.
20. Mackey M., L. Glass (1977). Oscillation and Chaos in Physiological Control Systems, Science, New series, 197(4300), 287-289.
21. Markowitz S., M. Bertagnolli (2009). Molecular Basic of Colorectal Cancer, New England Journal of Medicine, 361, 2449-2460.
22. Matlab (2007). The MathWorks, Inc. Retrieved from http://www.mathworks.com.
23. Neimark Yu. I., P. S. Landa (1992). Stochastic and Chaotic Oscillations, Kluwer Acad Publishers, Dordrecht.
24. Nenov M., S. Nikolov, G. Genova (2012). A Computational Approach to Identifying miRNAs Implicated in *Drosophila* Neurodevelopment, Int J Bioautomation, 16(1), 1-12.
25. Nicolas P., K. Kim, D. Shibata, S. Tavare (2007). The Stem Cell Population of the Human Colon Crypt: Analysis via Methylation Patterns, PLoS Computational Biology, 3(3), e28.
26. Nikolov S. (2008). Dynamics and Complexity in a Time Delay Model of RNA Silencing with Periodic Forcing, Int J Bioautomation, 10, 1-12.
27. Nikolov S. (2008). Stability and Bifurcation Behaviour of Genetic Regulatory Systems with Two Delays, Comptes rendus de l'Academie bulgare des Sciences, 61(5), 585-594.
28. Nikolov S., X. Lai, O. Wolkenhauer, J. Vera (2009). Time Delay and Epo Dose Modulation in a Multilevel Model for Erythropoiesis, Int J Bioautomation, 12, 53-69.
29. Nikolov S., M. Ullah, M. Nenov, J. V. Gonzales, P. Raasch, O. Wolkenhauer (2013). Modeling Colorectal Cancer: A Stability Analysis Approach, In: Medical Advancements in Aging and Regenerative Technologies: Clinical Tools and Applications, Daskalaki A. (Ed.), IGI Global, 53-75.
30. Nikolov S., O. Wolkenhauer, J. Vera (2014). Tumors as Chaotic Attractors, Molecular BioSystems, 10(2), 172-179.
31. Pyragas K. (1992). Continuous Control of Chaos by Self-controlling Feedback, Physics Letters A, 170, 421-428.
32. Redmond B., V. LeBlanc, A. Longtin (2002). Bifurcation Analysis of a Class of First-order Nonlinear Delay Differential Equations with Reflectional Symmetry, Physica D, 166, 131-146.
33. Robert C., K. Alligood, E. Ott, J. Yorke (2002). Explosions of Chaotic Sets, Physica D, 144(1-2), 44-61.
34. Sjoblom T., S. Jones, L. D. Wood, D. W. Parsons, J. Lin, T. D. Barber, D. Mandelker, R. J. Leary, J. Ptak, N. Silliman, S. Szabo, P. Buckhaults, C. Farrell, P. Meeh, S. D. Markowitz, J. Willis, D. Dawson, J. K. Willson, A. F. Gazdar, J. Hartigan, L. Wu, C. Liu, G. Parmigiani, B. H. Park, K. E. Bachman, N. Papadopoulos, B. Vogelstein, K. W. Kinzler, V. E. Velculescu (2006). The Consensus Coding Sequences of Human Breast and Colorectal Cancers, Science, 314, 268-274.
35. Siegmund K., P. Marjoram, S. Tavare, D. Shibata (2009). Many Colorectal Cancers are "Flat" Clonal Expansion, Cell Cycle, 8(14), 2187-2193.
36. Smallbone K., B. Corfe (2014). A Mathematical Model of the Colon Crypt Capturing Compositional Dynamic Interaction between Cell Types, Int J Experimental Pathology, 95, 1-7.

37. Sproull F., C. David (1979). Stem Cell Growth and Differentiation in Hydra Attenuata. I. Regulation of the Self-renewal Probability in Multiclone Aggregates, J Cell Science, 38, 155-169.
38. Stein U., P. Schlag (2007). Clinical, Biological, and Molecular Aspects of Metastasis in Colorectal Cancer, Recent Results Cancer Research, 176, 61-80.
39. Walther A., E. Johnstone, C. Swanton, R. Midgley, I. Tomlinson, D. Kerr (2009). Genetic Prognostic and Predictive Markers in Colorectal Cancer, Nature Reviews Cancer, 9, 489-499.
40. Watt F., L. Hogan (2000). Out of Eden: Stem Cells and Their Niches, Science, 287, 1427-1430.
41. Wodarz D., N. Komarova (2005). Computational Biology of Cancer: Lecture Notes and Mathematical Modelling, Singapore, World Scientific.
42. Wodarz D. (2007). Effect of Stem Cell Turnover Rates on Protection against Cancer and Aging, J Theoretical Biology, 245, 449-458.
43. Wolpin B., R. Mazer (2008). Systemic Treatment of Colorectal Cancer, Gastroenterology, 134, 1296-1310.
44. Zhao R., F. Michor (2013). Patterns of Proliferative Activity in the Colonic Crypt Determine Crypt Stability and Rates of Somatic Evolution, PLoS Computational Biology, 9(6), e1003082.

Appendix

Centre manifold reduction for first order DDEs

Here we explain the most essential facts relevant to our work about using the normal form method and the center manifold theorem [4, 31]. Without loss of generality we consider one-dimensional autonomous DDE of the form (7).

We begin with construction of the centre manifold for Eq. (7). In standard notation [8] Eq. (7) can be rewritten as

$$\dot{u}(t) = Lu_t + F(u_t), \tag{A.1}$$

where $u_t = x(t+\theta) \in R^{1+p}$, $-h \le \theta \le 0$, $C = C([-h, 0], R^{1+p})$, $L: C \to R^1$ is a bounded linear operator and $F: R \times C \to R^{1+p}$ is some smooth nonlinearity with $F(0) = 0$ and $DF(0) = 0$. Here Eq. (A.1) should be viewed as a suspended system where the p parameters are included as dynamic variables with trivial dynamics. For our purposes, the dimension p of parameter space for the suspended system will equal 1 or 2, depending on the bifurcation under study. The linearization of Eq. (A.1) about the some equilibrium is given by

$$\dot{u}(t) = Lu_t,\ t \ge 0. \tag{A.2}$$

Since L is a bounded linear operator, it follows from Riesz's representation theorem that L can be written by Riemann-Stieltjes integral

$$L\varphi = \int_{-\tau}^{0} [d\eta(\theta)]\varphi(\theta),\ \varphi = (\varphi_1(\theta))^{\mathrm{T}} \in C, \tag{A.3}$$

where $\eta(\theta)$, $-\tau \le \theta \le 0$, is a (1 + p)×(1 + p) matrix function whose elements are bounded variation. We note that in case of discrete delays the function $\eta(\theta)$ (which express L as an integral operator) is just the Dirac delta "function", i.e.

$$x(t-\tau) = \int_{-\tau}^{0} \delta(\theta+\tau) x_t d\theta, \quad \text{and} \quad \delta(\theta) = \begin{cases} 0, & \theta \neq 0 \\ 1, & \theta = 0 \end{cases}.$$

We may then rewrite Eq. (A.2) in the following form

$$\dot{u}(t) = \int_{-\tau}^{0} \left[d\eta(\theta) \right] u(t+\theta), \; t \ge 0. \tag{A.4}$$

If $R^{(1+p)*}$ is a space of row vectors, then we define $C' = C\left([0, \tau], R^{(1+p)*} \right)$. Hence, the transpose of Eq. (A.4) is

$$\dot{u}(t) = -\int_{-\tau}^{0} u(t-\theta) \left[d\eta(\theta) \right], \quad t \ge 0, \quad u_0 = \psi \in C'. \tag{A.5}$$

For $\phi \in C$ and $\psi \in C'$, the following bilinear form is defined

$$\langle \psi, \phi \rangle = \psi(0)\phi(0) - \int_{-\tau}^{0} \int_{0}^{\theta} \psi(\zeta - \theta) [d\eta(\theta)] \phi(\zeta) d\zeta, \tag{A.6}$$

where $\psi(0)\phi(0)$ represents the usual scalar (dot) product of two vectors.

Since Eq. (A.1) has p components with trivial dynamics, then the characteristic equation corresponding to Eq. (A.2) always has p eigenvalues on the imaginary axis. Thus, at a bifurcation, 1 + p eigenvalues on the imaginary axis exist and we assume that all other roots of characteristic equation are with negative real part. Then there an (1 + p)-dimensional centre subspace $P \subset C$ for Eq. (A.4) exists which is invariant under the semi-flow for Eq. (A.2). We will denote a basis for P by the (1 + p)×(1 + p) matrix Φ (all columns of are the basis vectors). There is corresponding (1 + p)-dimensional subspace P' of C' with solutions to the transposed Eq. (A.5). We will denote also a basis for P' by the (1 + p)×(1 + p) matrix Ψ′. Because the (1 + p)×(1 + p) matrix $\langle \Psi', \Phi' \rangle$ is always non-singular [7] then a new basis Ψ for P' by $\Psi = \langle \Psi', \Phi \rangle^{-1} \Psi'$, where Ψ is normalized by $\langle \Psi, \Phi \rangle = I$. At a point in parameter space (where the linear Eq. (A.2) possesses one eigenvalue with zero real part), there exists a splitting of the space $C = P \oplus Q$, where Q is infinite dimensional and invariant under the flow associated with Eq. (A.2). Further, it can be shown using integral manifold techniques [8] that there exists an (1 + p)-dimensional centre manifold M_F for Eq. (A.1) given by

$$M_F = \left\{ \varphi \in C : \varphi = \Phi z + h(z, F), \; z \text{ in a neighbourhood of zero in } R^{1+p} \right\}, \tag{A.7}$$

where $h(z, F) \in Q$ for each z and is a C' function of z. The flow on this centre manifold is

$$u_t = \Phi z(t) + h\left(z(t), F\right), \tag{A.8}$$

and z satisfies the ordinary differential equation

$$\dot{z} = Bz + \Psi(0)F\left(\Phi z + h(z, F)\right). \tag{A.9}$$

In Eq. (A.9), $\Psi(0)$ is determined from the solution of the equation adjoined to Eq. (A.1) and B is the $(1 + p)\times(1 + p)$ matrix of eigenvalues of Eq. (A.2) with null real part, i.e. matrix B satisfies the relation

$$\frac{d\Phi}{d\theta} = \Phi B. \tag{A.10}$$

The flow of Eq. (A.9) approximates well the long term behavior of the flow of the full nonlinear system (A.1) near the origin.

Assoc. Prof. Svetoslav G. Nikolov, Ph.D., D.Sc.
E-mail: s.nikolov@imbm.bas.bg

Svetoslav Nikolov's research and educational interests are in the fields of mathematical modelling, nonlinear dynamics and bifurcation analysis of systems in cell biology. He received his M.Sc. in Mechanical Engineering from the Technical University of Sofia, Bulgaria, in 1994; Ph.D. degree from the Institute of Mechanics and Biomechanics (IMech) − Bulgarian Academy of Science, in 1999, and D.Sc. degree from University of Transport, Sofia, in 2013. Since 2005 he has been an Associate Professor at IMech and since 2012 − a Professor at University of Transport, Sofia, Bulgaria.

Prof. Dr. Olaf Wolkenhauer, Ph.D.
E-mail: olaf.wolkenhauer@uni-rostock.de

Prof. Dr. Olaf Wolkenhauer obtained his first degree in Control Engineering, followed by a Ph.D. at the UMIST in Manchester, UK and a joint position with the Department of Biomolecular Sciences. Since 2004 he has occupied the Chair in Systems Biology & Bioinformatics at the University of Rostock, Germany (www.sbi.uni-rostock.de). His research interests are in systems biology and bioinformatics, focussing on dynamical aspects of inter- and intra-cellular processes and tissue organization.

Assoc. Prof. Julio Vera, Ph.D.
E-mail: jullio.vera-gonzalez@uk-erlangen.de

Assoc. Prof. Julio Vera studied Applied Physics and obtained a doctorate in Molecular Biology and Biochemistry at the University of La Laguna, Spain (1999-2005). He was post-doctoral researcher and research group leader at the Department of Systems Biology and Bioinformatics, Uni-Rostock, Germany (2005-2013). Since May 2014 he is an Associated Professor in Systems Tumor Immunology at the University Hospital of Erlangen and the FAU − University of Erlangen-Nuremberg, Germany. He works in mathematical modelling of cancer signaling, miRNA and gene networks.